Photobiomodulation—Original Research

Effects of Home Photobiomodulation Treatments on Cognitive and Behavioral Function, Cerebral Perfusion, and Resting-State Functional Connectivity in Patients with Dementia: A Pilot Trial

Linda L. Chao, PhD[1–3]

Abstract

Objective: To examine the effects of transcranial and intranasal photobiomodulation (PBM) therapy, administered at home, in patients with dementia.

Background: This study sought to replicate and build upon a previously published case series report describing improved cognitive function in five patients with mild-to-moderate dementia after 12 weeks of transcranial and intranasal near-infrared (NIR) PBM therapy.

Materials and methods: Eight participants (mean age: 79.8 ± 5.8 years old) diagnosed with dementia by their physicians were randomized to 12 weeks of usual care (UC, $n=4$) or home PBM treatments ($n=4$). The NIR PBM treatments were administered by a study partner at home three times per week with the Vielight Neuro Gamma device. The participants were assessed with the Alzheimer's Disease Assessment Scale-cognitive (ADAS-cog) subscale and the Neuropsychiatric Inventory (NPI) at baseline and 6 and 12 weeks, and with arterial spin-labeled perfusion magnetic resonance imaging (MRI) and resting-state functional MRI at baseline and 12 weeks.

Results: At baseline, the UC and PBM groups did not differ demographically or clinically. However, after 12 weeks, there were improvements in ADAS-cog (group × time interaction: $F_{1,6} = 16.35$, $p = 0.007$) and NPI (group × time interaction: $F_{1,6} = 7.52$, $p = 0.03$), increased cerebral perfusion (group × time interaction: $F_{1,6} = 8.46$, $p < 0.03$), and increased connectivity between the posterior cingulate cortex and lateral parietal nodes within the default-mode network in the PBM group.

Conclusions: Because PBM was well tolerated and associated with no adverse side effects, these results support the potential of PBM therapy as a viable home treatment for individuals with dementia.

Keywords: dementia, Alzheimer's disease, photobiomodulation, LED, neuroimaging

Introduction

ALZHEIMER'S DEMENTIA (AD) is a global health problem with no cure.[1] Current AD medications have considerable side effects and only offer limited symptomatic relief.[2] Because AD is characterized by neurofibrillary tangles of hyperphosphorylated tau and Aβ plaques,[3] recent AD trials have focused on anti-Aβ_{42} and anti-tau disease-modifying strategies in the earliest stages of the disease. Consequently, limited attention has been devoted to treatments that manage cognitive impairment and behavioral symptoms in a growing population of patients affected by more advanced stages of the disease.

Photobiomodulation (PBM) uses radiant light energy to modify biological functions and/or induce a therapeutic effect.[4,5] PBM can be delivered transcranially to target the brain parenchyma in humans because research with cadavers suggests that near-infrared (NIR) light can penetrate the scalp, skull, and meninges[6] to a depth of ~ 40 mm.[7] The first aim of this study is to replicate and extend the behavioral findings of previous study that reported improved cognitive function in five dementia patients after 12 weeks of transcranial and intranasal NIR PBM treatments.[8]

Many researchers believe that the beneficial effects of PBM may be explained by increases in cerebral blood flow

[1]Center for Imaging of Neurodegenerative Diseases, San Francisco VA Medical Center, San Francisco, California.
Departments of [2]Radiology and Biomedical Imaging and [3]Psychiatry, University of California, San Francisco, San Francisco, California.

(CBF) and oxygen consumption.[9–12] Therefore, the second aim of this study is to investigate the impact of transcranial and intranasal NIR PBM on CBF in participants with dementia.

The default-mode network (DMN) is one of the best-studied resting-state networks thought to represent the maintenance of baseline human cognition and metabolic equilibrium.[13] The DMN consists of a group of strongly interconnected[14] brain regions [i.e., posterior cingulate cortex (PCC), precuneus, inferior parietal, medial prefrontal cortex, and medial temporal cortex[15]] that show increased activity in task-free state compared to cognitively demanding task and synchronized activity at rest.[16] Because functional connectivity in the DMN is sensitive to AD pathology across the clinical spectrum, from mild cognitive impairment (MCI), considered a prodromal stage of AD,[17–19] to the later stages of AD,[20–23] the light-emitting diodes (LEDs) of the PBM device utilized in this and Saltmarche et al.'s[8] study were specifically engineered to target nodes of the DMN. Therefore, the final aim of this study was to examine the effect of transcranial and intranasal PBM on DMN connectivity in participants with dementia.

Materials and Methods

Participants

Individuals diagnosed with dementia or AD by their physicians and their study partners (i.e., spouses or children) were enrolled as dyads for the study. The research was approved by the Institutional Review Board at the University of California, San Francisco, and at the San Francisco Veterans Affairs Medical center. Written informed consent was obtained from all participants (or their legally authorized representatives) and study partners in accordance with the Declaration of Helsinki. Participants were compensated $50 for undergoing the neuroimaging procedures. Study partners were not paid for participation in the study.

Participants were either randomized to a Usual Care (UC) group, which engaged in their usual activities for 12 weeks, or a PBM group, which received PBM treatments at home for 3 days a week for 12 weeks. PBM study partners were trained how to position the PBM device, administer PBM treatments, and control, clean and maintain PBM device in a single session. One week after the training, the study partners were asked to demonstrate their ability to correctly position the device and administer PBM treatments to the participants. Mistakes were corrected and study partners were retrained when necessary. The study partners logged the PBM treatments throughout the 12 weeks in a home treatment diary and were contacted by the study staff twice a month to assess for adverse events.

UC participants had the option of receiving 12 weeks of PBM treatments at home upon completion of the initial study procedures. The UC study partners were trained how to use and maintain the PBM device following an identical protocol as that used with the PBM study partners.

Study participants could continue their dementia medications during the trial. However, they were asked not to change or start new medication. Table 1 summarizes the demographic and clinical characteristics of the two groups at baseline.

TABLE 1. BASELINE CHARACTERISTICS OF STUDY SAMPLE

Characteristic[a]	PBM group	UC group
N	4	4
Age, years	80.5 ± 6.5	79.0 ± 5.9
Education, years	18.5 ± 1.9	18.0 ± 1.6
Gender, female	3 (75%)	2 (50%)
Race, white	4 (100%)	4 (100%)
Baseline MMSE	19.5 ± 7.0	22.3 ± 1.3
Prescribed dementia medication (number of patients)	Memantine (1) Donepezil (1)	Memantine (3) Donepezil (3)
Other prescribed medication (number of patients)	Tradazone (1) Citalopram (1) Losartan (2) Statins (2)	Quetiapine (1) Lorazepam (1)

[a]Mean ± SD for continuous variables and N (%) for categorical variables.

MMSE, Mini-Mental State Examination; PBM, photobiomodulation; SD, standard deviation; UC, usual care.

PBM device and treatment protocol

Table 2 summarizes the light parameters of the PBM device (Fig. 1) used in the study.

Cognitive and behavioral outcome measures

Cognitive and behavioral assessments were performed at baseline and 6 and 12 weeks. UC participants who chose to undergo 12 weeks of PBM treatments were also assessed at 18 and 24 weeks. The Mini-Mental State Examination (MMSE)[24] was administered at baseline to obtain a brief measure of global cognitive status.

The Alzheimer's Disease Assessment Scale-cognitive (ADAS-cog) subscale[25] was used to assess cognitive function. The ADAS-cog, one of the most common primary outcome measures in dementia drug treatment trials, is an 80-point test that includes direct assessment of learning (word list), naming (objects), following commands, constructional praxis (figure copying), ideational praxis (mailing a letter), orientation (person, time, place), recognition memory, and remembering test instructions. The ADAS-cog has good test-retest reliability (above 0.9)[26] and internal consistency (Cronbach's alpha >0.8).[26]

Dementia-related behaviors were assessed with the Neuropsychiatric Inventory[27] (NPI), a 144-point informant-based questionnaire that asks about 12 behavioral domains common in dementia, including frequency, severity, and impact on caregiver distress. The NPI frequency × severity total score (NPI-FS) was used as a summary measure. The NPI has good test-retest reliability (0.79–0.86) and internal consistency (Cronbach's alpha, 0.87–0.88).[27]

Neuroimaging measures

Neuroimaging assessments were performed at baseline and week 12 on a Siemens 3 Tesla Trio Scanner equipped with a 32-channel receiver head coil. The imaging protocol included a structural T1-weighted 3D Magnetization Prepared Rapid Gradient Echo image [repetition time (TR)/echo time (TE)/inversion time (TI) = 2500/2.98/1100 msec, $1.0 \times 1.0 \times 1.0$ mm^3

TABLE 2. PARAMETERS OF THE VIELIGHT NEURO GAMMA DEVICE

Source	Light-emitting diode (LED)
Wavelength, nm	810, Non-laser
Power output, mW	100 (posterior transcranial LEDs); 75 (anterior transcranial LED); 25 (intranasal LED)
Power density per LED, mW/cm^2	100 (posterior transcranial LEDs); 75 (anterior transcranial LED); 25 (intranasal LED)
Pulse frequency, Hz	40
Pulse duty cycle, percentage	50
Duration of each treatment session, min	20
Frequency of treatment	3 times per week
Beam spot size, cm^2	≈1
Energy delivered, J	60 (posterior transcranial headband); 45 (anterior transcranial headband); 15 (intranasal LED)
Energy density per LED, J/cm^2	60 (posterior transcranial headband); 45 (anterior transcranial headband); 15 (intranasal LED)
Dose of each treatment session, J	240
Cumulative energy density per LED, per week	540 (transcranial headset); 135 (transcranial headset); 45 (intranasal LED)
Cumulative dose per week, J	720

resolution] and arterial spin-labeled (ASL) magnetic resonance imaging (MRI), a noninvasive technique where arterial water is magnetically labeled and used as an endogenous tracer to measure CBF.[28] The ASL MRI data were acquired with the following echo-planar imaging (EPI) sequence: inversion time of arterial spins: 700 msec, total transit time of the spins: 1900 msec, tag thickness: 100 mm, tag to proximal slice gap: 25.4 mm, repetition time: 3400 msec, echo time: 13 msec, field of view: 256 mm, 64×64 matrix, and 24 four-mm thick axial slices (52 tag + control image pairs, time lag between slices: 22.5 msec). Finally, we acquired resting-state functional connectivity data with an 8-min 12-sec EPI sequence (140 time points, TR = 3000 msec, TE = 30 msec, and flip angle = 80°; number of slices = 48; slice thickness = 3.3 mm and spatial resolution = 3.3 × 3.3 × 3.3 mm^3; and matrix = 64 × 64).

Image analysis

ASL MRI data processing included the following: motion correction, aligning each ASL frame to the first frame using a rigid body transformation, and least-squares fitting using SPM8. Perfusion weighted images were computed as the difference between the mean of tagged and untagged ASL data sets. To account for signal decay during acquisition and allow for intensities in meaningful physiological units, the perfusion weighted images were intensity scaled. After geometric distortion correction, the ASL images were aligned to structural T1-weighted images. To estimate CBF from gray matter (GM) and minimize the effects of the lower perfusion in white matter (WM) on the CBF estimates, a partial volume correction was performed, which assumed GM CBF is 2.5 times greater than in WM.

FreeSurfer (version 5.1.0) generated anatomical regions of interest (ROIs) were used to analyze the CBF data. Mean GM CBF from the right and left superior frontal, superior parietal, and supramarginal cortex, which correspond to brain regions targeted by the transcranial LEDs of the PBM device (Fig. 2), were extracted for all subjects. Mean GM CBF values from the precentral gyrus parcel (i.e., primary motor cortex) were used as a control for the meta-ROI because this brain region is least likely to be affected by dementia-related neuropathology.

FIG. 1. Vielight Neuro Gamma device (left) and photograph illustrating positions of the device LEDs during treatment (right). Figure courtesy of Vielight, Inc. LED, light-emitting diode.
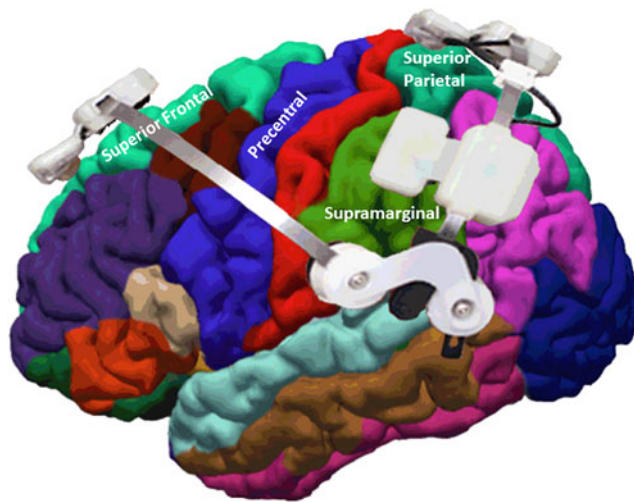
FIG. 2. Approximate position of the Vielight Neuro Gamma transcranial LEDs on the FreeSurfer ROIs. The precentral ROI was used as a control region in analysis of the perfusion data. ROI, regions of interest.

The temporal and occipital lobes were not included in analysis of the ASL perfusion data because of artifacts in EPI data from the temporal regions[29,30] and because the LEDs on the PBM device did not target these brain regions.

The functional connectivity data were pre-processed and analyzed using SPM12 software.[31] All functional images were slice-timing corrected and realigned to the first volume using a six-parameter rigid body transformation. The mean image generated was spatially normalized into standard stereotactic space using the Montreal Neurological Institute (MNI) EPI template. Computed transformation parameters were applied to all functional images, interpolated to iso-tropic voxels of 2mm^3, and the resulting images were smoothed using an 8-mm full-width half-maximum isotropic Gaussian Kernel.

Statistical analysis

Statistical Analysis was carried out using SPSS version 25 (IBM Corp., Armonk, NY). Demographic and clinical characteristics of the PBM and UC groups were compared using t-tests for continuous variables and Fisher's exact test for categorical variables. A repeated-measures analysis of variance was used to analyze the between-group differences in the ADAS-cog and NPI-FS, with time (baseline and 6 and 12 weeks) as the within-subject factor. A repeated-measures multi-variate analysis of variance was used to analyze the between-group differences in ASL MRI perfusion data, with time and ROI (superior frontal, superior parietal, and su-pramarginal) as the within-subject factors.

Analysis of the functional connectivity data was performed with the CONN-functional MRI Functional Connectivity toolbox v 17.[32] Default pre-processing parameters were used to address the possible confounding effect of head motion artifacts and WM, and cerebral spinal fluid (CSF) blood oxygen level-dependent (BOLD) signal.[32] BOLD signal noise from the WM and CSF was characterized with the principal component-based noise-correction ''Comp-Cor'' method utilized in the CONN toolbox.[33] Band-pass filtering was performed with a frequency window of 0.008–0.09 Hz.

ROI-to-ROI functional connectivity maps were created for each participant. The mean BOLD time series was computed across all voxels within each ROI. Bivariate-regression analyses were used to determine the linear association of the BOLD time series between each pair of sources. Each scan was Hanning weighted.[32]

A pre-defined spherical ROI (radius: 10 mm) was chosen as the seed to create connectivity maps of the DMN in the PCC region, MNI coordinates 1, −61, and 38, based on prior studies. For ROI-to-ROI analyses, a peak voxel threshold of $p \leq 0.001$ and a cluster extent threshold of $p \leq 0.05$ were set for bidirectional explorations of connectivity.

Results

Baseline demographic and clinical characteristics

Table 1 summarizes the baseline demographic and clinical characteristics of the PBM and UC groups. There were no differences in age ($t=0.34$, $df=6$, $p=0.74$), years of education ($t=0.40$, $df=6$, $p=0.71$), or MMSE ($t=0.77$, $df=6$, $p=0.47$) at baseline.

Behavioral outcomes: ADAS-Cog and NPI-FS

Table 3 and Fig. 3 summarize the changes in ADAS-cog and NPI-FS scores from baseline to weeks 6 and 12. Higher scores on both measures indicate poorer cognitive function and more numerous/severe dementia-related behaviors.

TABLE 3. COGNITIVE, BEHAVIORAL, AND PERFUSION OUTCOME MEASURES BY GROUP AND TIME

|	Baseline	Week-6	Week-12
ADAS-cog[a]			
UC	32.1 (0.3)	34.8 (1.2)	39.2 (2.6)
PBM	37.5 (5.5)	35.7 (4.7)	32.3 (4.8)
NPI-FS[a]			
UC	10.5 (1.8)	14.5 (3.1)	20.3 (3.5)
PBM	35.0 (11.6)	22.8 (4.0)	13.5 (2.0)
Total perfusion[b,c]			
UC	1.20 (0.11)	—	0.91 (0.16)
PBM	0.89 (0.11)	—	1.22 (0.16)
Superior frontal perfusion[c]			
UC	0.69 (0.22)	—	0.61 (0.19)
PBM	0.75 (0.04)	—	0.77 (0.10)
Superior parietal perfusion[c]			
UC	1.04 (0.14)	—	1.02 (0.10)
PBM	0.75 (0.14)	—	1.41 (0.33)
Supramarginal perfusion[c]			
UC	1.87 (0.20)	—	1.09 (0.24)
PBM	1.16 (0.22)	—	1.48 (0.21)

Values are mean (SEM).
[a]Lower scores = better.
[b]Values are averaged across superior frontal, superior parietal, and supramarginal regions of interest.
[c]Values are normalized to precentral motor perfusion values.
ADAS-cog, Alzheimer's Disease Assessment Scale-cognitive; NPI-FS, Neuropsychiatric Inventory frequency severity; PBM, photobio-modulation; SEM, standard error of the mean; UC, usual care.
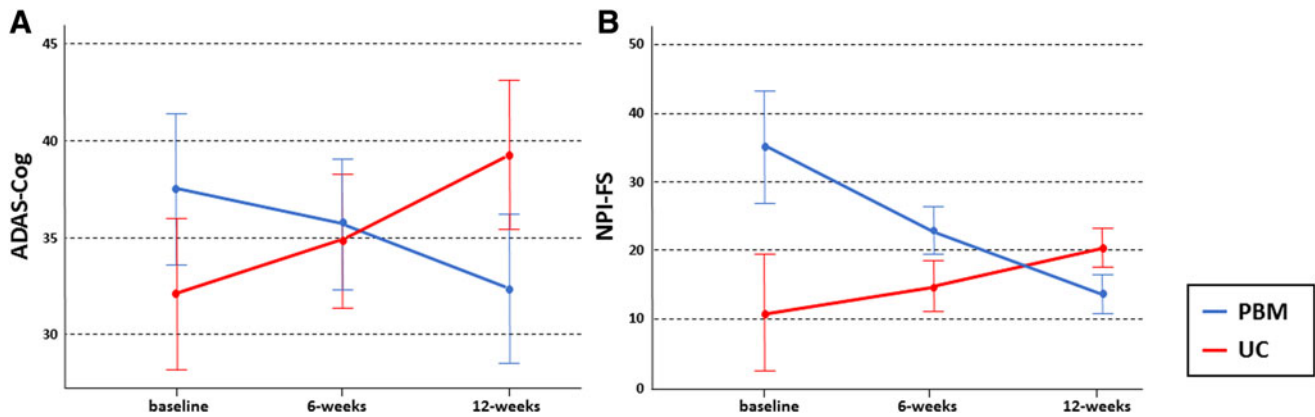
FIG. 3. Mean (±SEM) ADAS-cog **(A)** and NPI-FS **(B)** scores in the PBM (blue line) and UC (red line) groups by time. Lower scores on both measures indicate better function. ADAS-cog, Alzheimer's Disease Assessment Scale-cognitive; NPI-FS, Neuropsychiatric Inventory frequency severity; PBM, photobiomodulation; SEM, standard error of the mean; UC, usual care.

There were no group differences in ADAS-cog ($t = 0.98$, $df = 6$, $p = 0.37$) at baseline; however, there was a trend for lower NPI-FS scores in the UC compared to the PBM group ($t = 2.08$, $df = 6$, $p = 0.08$). After 12 weeks, the ADAS-cog (group × time interaction: $F_{1,6} = 16.35$, $p = 0.007$) and NPI-FS (group × time interaction: $F_{1,6} = 7.52$, $p = 0.03$) improved in the PBM group, but declined in the UC group.

Imaging outcome: ASL perfusion

Table 3 summarizes the changes in ASL perfusion from baseline to week 12. After 12 weeks, there was greater CBF in the PBM group compared to the UC group (group × time interaction: $F_{1,6} = 8.46$, $p < 0.03$), particularly in the parietal ROIs (group × time × ROI interaction: $F_{1,6} = 8.93$, $p = 0.02$, Fig. 4B, C).

Imaging outcome: DMN activity

Contrasts of DMN activity in the PBM versus UC at baseline and week 12 did not reach significance. However, there was increased connectivity between a seed in the PCC (hub of DMN: 1, −61, 38) and the lateral parietal (LP) cortex in the PBM group from baseline and week 12, and decreased connectivity in the UC group (Table 4; Fig. 5). There were

no significant relationships between the changes in ASL perfusion and functional connectivity.

Behavioral outcome in UC group after 12 weeks of PBM

There was a trend of improvement on the ADAS-Cog ($F_{4,8} = 3.45$, $p = 0.06$) after 12 weeks of PBM in the three UC participants who chose to undergo 12 weeks of home PBM treatments after completing the initial study (Fig. 6).

Discussion

The first finding of this study is that scores on the ADAS-cog improved after 12 weeks in the PBM group, but declined in the UC group. Scored according to the number of errors committed, a higher ADAS-cog score reflects poorer cognitive function. Saltmarche et al.[8] reported a mean change from baseline of −7.40 points (i.e., improvement) after 6 weeks and −6.73 points after 12 weeks of PBM. In this study, the PBM group improved an average of −1.83 points after 6 weeks and −5.18 points after 12 weeks of treatments. Although the sample sizes in this and Saltmarche et al.'s[8] study were small, it is noteworthy that these PBM-related ADAS-cog improvements are larger than what has been reported in previous pharmacological trials of donepezil (10 mg/day)
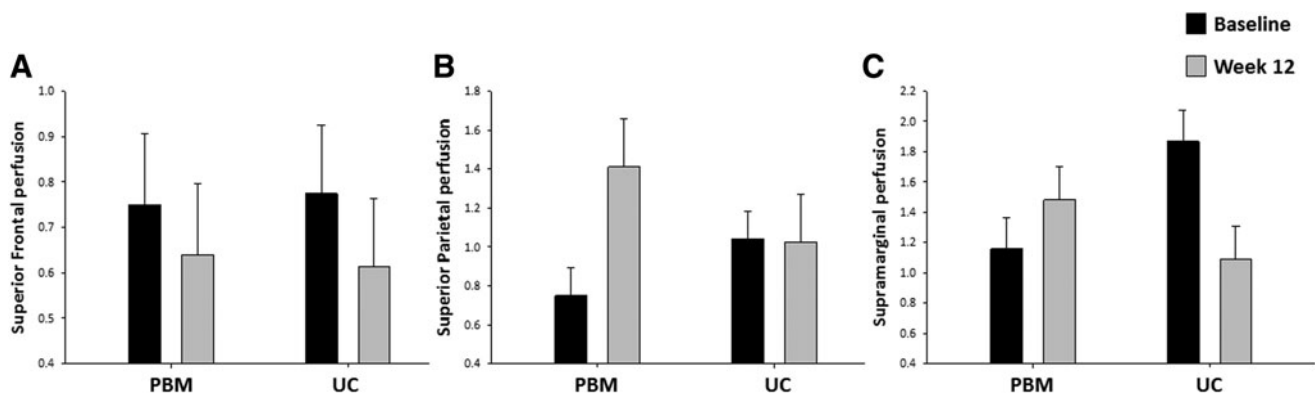
FIG. 4. Arterial spin-labeled perfusion values, normalized to the precentral ROI, from the superior frontal **(A)**, superior parietal **(B)**, and supramarginal **(C)** ROIs at baseline (black bar) and week 12 (gray bar) by group. Error bars are SEM. ROIs, regions of interest; SEM, standard error of the mean.

TABLE 4. STRENGTH OF CONNECTIVITY BETWEEN THE POSTERIOR CINGULATE CORTEX (SEED)
AND LATERAL PARIETAL CORTEX BY GROUP AND TIME

	PBM		UC	
	Baseline	Week 12	Baseline	Week 12
PCC–left LP	$T(3)=4.25$ $P_{unc}=0.02$ $P_{FDR}=0.07$	$T(3)=14.15$ $P_{unc}=0.0008$ $P_{FDR}=0.004$	$T(3)=6.88$ $P_{unc}=0.006$ $P_{FDR}=0.02$	$T(3)=3.86$ $P_{unc}=0.03$ $P_{FDR}=0.08$
PCC–right LP	$T(3)=3.98$ $P_{unc}=0.03$ $P_{FDR}=0.07$	$T(3)=11.17$ $P_{unc}=0.002$ $P_{FDR}=0.004$	$T(3)=8.34$ $P_{unc}=0.004$ $P_{FDR}=0.02$	$T(3)=5.04$ $P_{unc}=0.02$ $P_{FDR}=0.08$

LP, lateral parietal; PBM, photobiomodulation; PCC, posterior cingulate cortex; UC, usual care.

in AD patients (mean difference: −2.67 improvement, 95% confidence interval: −3.31 to −2.02).[34]

The second finding of this study is that scores on the NPI-FS improved in the PBM group after 12 weeks, but declined in the UC group. Saltmarche et al.[8] did not formally quantify behavioral symptoms; however, they documented qualitative feedback from the patients and caregivers, noting improvements in quality of life, functional abilities (i.e., decreased incontinence and increased mobility), better sleep, fewer angry outbursts, and less anxiety and wandering after the PBM treatments. A summary measure of the individual domain scores: higher NPI-FS scores reflect more severe/more frequent dementia-related behavior. In this study, the PBM group improved an average of −12.3 points on the NPI-FS after 6 weeks and −22.8 points after 12 weeks of treatments. By comparison, previous pharmacological trials of donepezil reported no difference from placebo on behavioral symptoms measured by the NPI[34] and no difference on quality of life.[34]

Importantly, there were no adverse effects associated with the PBM treatments in this or Saltmarche et al.'s study.[8] In contrast, many of the Food and Drug Administration-approved pharmacological treatments for dementia have been associated with substantial side effect burden,[35–38] such as diarrhea, vomiting, nausea, and fatigue.

AD is characterized by decreased regional cerebral blood flow (rCBF)[39] and reductions in regional cerebral metabolic rate of glucose metabolism (rCMRglc),[40] most notably in the PCC, precuneus, and bilateral parietal lobe.[41–46] Cholinesterase inhibitors, such as donepezil and rivastigmine, have been reported to improve rCBF[47–49] and rCMRglc[50] in patients with AD. The third finding of this study is that cerebral perfusion increased after 12 weeks in the PBM group compared to the UC group. This finding is consistent with previous reports of PBM-related increases in local CBF,[51] oxygen consumption,[52] total hemoglobin, a proxy for increased rCBF,[53] rCBF,[54] and increased oxygenated/decreased deoxygenated hemoglobin concentrations.[11]

Interestingly, the PBM-related increases in perfusion were most prominent in the parietal ROIs. This may relate to the fact that the PBM device used in this study had three transcranial LED clusters over the parietal lobe and only one transcranial LED cluster over the frontal lobe. This finding may also be explained by the report that NIR light penetrates more deeply through the parietal lobe compared to the frontal lobe.[7]

Similar to decreases in rCBF, connectivity changes in the DMN have been described in populations at risk for AD[17–19] as well as in patients with AD.[20–23] In fact, DMN activity changes seen in AD are similar to those found in
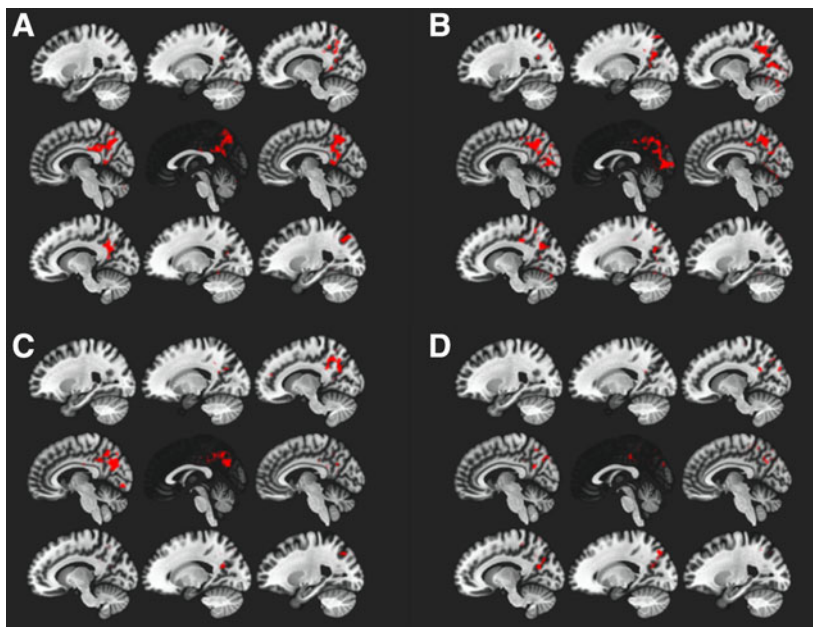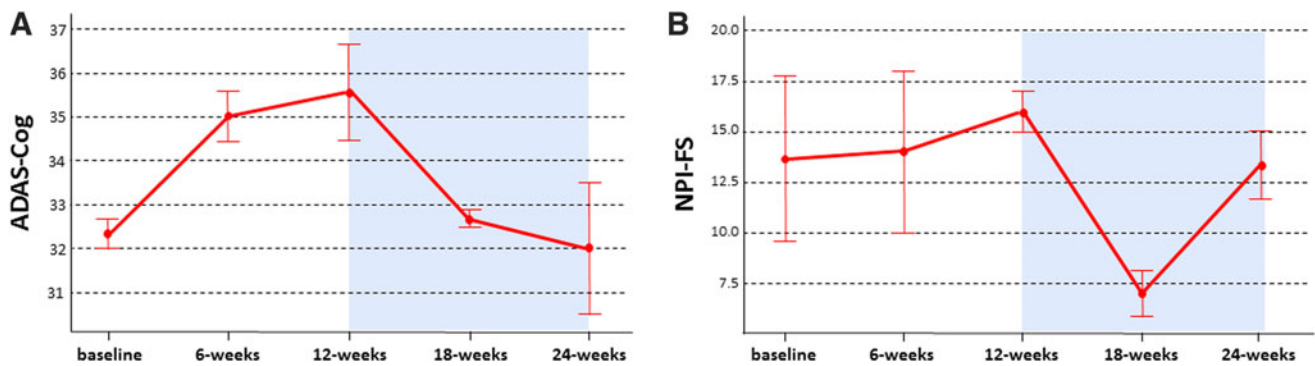

FIG. 5. Default-mode network activity in the PBM group—(A) baseline and (B) week 12 and in the usual care group—(C) baseline and (D) week 12. The posterior cingulate cortex (1, −61, and 38) was used as seed in the analysis; Height threshold: P_{unc} < 0.001; cluster threshold P_{FDR} < 0.05.

FIG. 6. Mean (±SEM) ADAS-cog **(A)** and NPI-FS **(B)** scores in three Usual Care patients before and after (shaded blue) using PBM device at home. Lower scores on both measures indicate better function. ADAS-cog, Alzheimer's Disease Assessment Scale-cognitive; NPI-FS, Neuropsychiatric Inventory frequency severity; PBM, photobiomodulation.

fluorodeoxyglucose positron emission tomography studies of resting-state brain metabolism, highlighting the major involvement of the PCC/precuneus region.[55,56] Because decreased DMN connectivity is a common finding in resting-state connectivity studies of AD,[23] it is significant that there was increased functional connectivity between the PCC and the LP nodes of the DMN in the PBM group after 12 weeks compared to the UC group. There have been reports of increased functional connectivity in the DMN after pharmacological treatments in mild-to-moderate AD patients.[57–61] There have also been studies that reported changes in functional connectivity after nonpharmacological intervention in patients with MCI.[62–64] To our knowledge, this is the first report of functional connectivity changes in dementia patients after a nonpharmacological intervention.

Because functional connectivity disturbances in the DMN overlap with patterns of amyloid deposition in patients with AD,[58,59,65] it is noteworthy that *in vitro* PBM has been reported to reduce $A\beta_{42}$ aggregates in cultured neuroblastoma cells challenged with $A\beta_{42}$,[66] amyloid load in amyloid-β protein precursor (AβPP) transgenic mice,[67] and Aβ plaque in an AβPP/presenilin 1 double mutant mouse model of AD.[68,69]

Although the PBM devices used in this and Saltmarche et al.'s[8] study were both manufactured by Vielight, some differences are worth noting: first, Saltmarche et al.[8] used the Neuro Alpha device, which pulsed 810 nm light at 10 Hz based on research suggesting that this particular combination of PBM produces the most robust neurobehavioral recovery in a mouse model of traumatic brain injury.[70,71] Based on a report suggesting that gamma oscillations stimulate the clearance of amyloid beta deposits,[72] Vielight, Inc. developed another device that pulsed 810 nm light at 40 Hz (i.e., Neuro Gamma device). Although this study used the Vielight Neuro Gamma device, because we did not quantify amyloid beta levels in study participants, it is unclear if the beneficial effects of PBM observed in the treatment group were accompanied by or associated with decreases in amyloid burden.

Limitations

This study had several limitations, including the small sample size, absence of a sham control group, the participants' diagnoses were not independently confirmed using the National Institute of Neurological and Communicative Disorders and Stroke and the Alzheimer's Disease and Related Disorders Association criterial,[73] and adherence to the home PBM treatment protocol was monitored solely through the treatment diaries. Future studies may consider remotely monitoring PBM device usage and tracking adherence by a radio-telemetry system.

Conclusions and Summary

The results from this and Saltmarche et al.'s[8] study support the potential of transcranial and intranasal PBM therapy as a safe home treatment for patients with dementia. Although there were no adverse events in this or Saltmarche et al.'s[8] study, larger, better controlled studies with biomarker-confirmed populations of AD patients will be necessary to confirm these findings.

Author Disclosure Statement

No competing financial interests exist.

References

1. Mayeux R, Stern Y. Epidemiology of Alzheimer disease. Cold Spring Harb Perspect Med 2012;2:a006239.
2. Mangialasche F, Solomon A, Winblad B, Mecocci P, Kivipelto M. Alzheimer's disease: clinical trials and drug development. Lancet Neurol 2010;9:702–716.
3. Perl DP. Neuropathology of Alzheimer's disease. Mt Sinai J Med 2010;77:32–42.
4. Karu TI. Mitochondrial signaling in mammalian cells activated by red and near-IR radiation. Photochem Photobiol 2008;84:1091–1099.
5. Rojas JC, Gonzalez-Lima F. Low-level light therapy of the eye and brain. Eye Brain 2011;3:49–67.
6. Tedford CE, DeLapp S, Jacques S, Anders J. Quantitative analysis of transcranial and intraparenchymal light penetration in human cadaver brain tissue. Lasers Surg Med 2015;47:312–322.
7. Jagdeo JR, Adams LE, Brody NI, Siegel DM. Transcranial red and near-infrared light transmission in a cadaveric model. PLoS One 2012;7:e47460.
8. Saltmarche AE, Naeser MA, Ho KF, Hamblin MR, Lim L. Significant improvement in cognition in mild to moderately severe dementia cases treated with transcranial plus intranasal photobiomodulation: case series report. Photomed Laser Surg 2017;35:432–441.
9. Cassano P, Petrie SR, Hamblin MR, Henderson TA, Iosifescu DV. Review of transcranial photobiomodulation for major depressive disorder: targeting brain metabolism,

inflammation, oxidative stress, and neurogenesis. Neuro-photonics 2016;3:031404.

10. Morries LD, Cassano P, Henderson TA. Treatments for traumatic brain injury with emphasis on transcranial near-infrared laser phototherapy. Neuropsychiatr Dis Treat 2015;11:2159–2175.

11. Tian F, Hase SN, Gonzales-Lima F, Liu H. Transcranial laser stimulation improves human cerebral oxygenation. Lasers Surg Med 2016;48:343–349.

12. Hamblin MR. Shining light on the head: photobiomodulation for brain disorders. BBA Clin 2016;6:113–124.

13. Gusnard DA, Raichle ME, Raichle ME. Searching for a baseline: functional imaging and the resting human brain. Nat Rev Neurosci 2001;2:685–694.

14. Greicius MD, Supekar K, Menon V, Dougherty RF. Resting-state functional connectivity reflects structural connectivity in the default mode network. Cereb Cortex 2009;19:72–78.

15. Raichle ME, Snyder AZ. A default mode of brain function: a brief history of an evolving idea. Neuroimage 2007;37: 1083–1090; discussion 1097–1099.

16. Mevel K, Chételat G, Eustache F, Desgranges B. The default mode network in healthy aging and Alzheimer's disease. Int J Alzheimers Dis 2011;2011:535816.

17. Sorg C, Riedl V, Mühlau M, et al. Selective changes of resting-state networks in individuals at risk for Alzheimer's disease. Proc Natl Acad Sci U S A 2007;104:18760–18765.

18. Bai F, Watson DR, Yu H, Shi Y, Yuan Y, Zhang Z. Abnormal resting-state functional connectivity of posterior cingulate cortex in amnestic type mild cognitive impairment. Brain Res 2009;1302:167–174.

19. Petrella JR, Sheldon FC, Prince SE, Calhoun VD, Doraiswamy PM. Default mode network connectivity in stable vs progressive mild cognitive impairment. Neurology 2011; 76:511–517.

20. Greicius MD, Srivastava G, Reiss AL, Menon V. Default-mode network activity distinguishes Alzheimer's disease from healthy aging: evidence from functional MRI. Proc Natl Acad Sci U S A 2004;101:4637–4642.

21. Wang K, Liang M, Wang L, et al. Altered functional connectivity in early Alzheimer's disease: a resting-state fMRI study. Human Brain Mapp 2007;28:967–978.

22. Zhang HY, Wang SJ, Xing J, et al. Detection of PCC functional connectivity characteristics in resting-state fMRI in mild Alzheimer's disease. Behav Brain Res 2009;197: 103–108.

23. Vemuri P, Jones DT, Jack CR, Jr. Resting state functional MRI in Alzheimer's Disease. Alzheimers Res Ther 2012;4:2.

24. Folstein MF, Folstein SE, McHugh PR. ''Mini-mental state''. A practical method for grading the cognitive state of patients for the clinician. J Psychiatr Res 1975;12:189–198.

25. Rosen WG, Mohs RC, Davis KL. A new rating scale for Alzheimer's disease. Am J Psychiatry 1984;141:1356–1364.

26. Weyer G, Erzigkeit H, Kanowski S, Ihl R, Hadler D. Alzheimer's disease assessment scale: reliability and validity in a multicenter clinical trial. Int Psychogeriatr 1997; 9:123–138.

27. Cummings JL. The Neuropsychiatric Inventory: assessing psychopathology in dementia patients. Neurology 1997;48: S10–S16.

28. Detre JA, Alsop DC. Perfusion magnetic resonance imaging with continuous arterial spin labeling: methods and clinical applications in the central nervous system. Eur J Radiol 1999;30:115–124.

29. Chen NK, Dickey CC, Yoo SS, Guttmann CR, Panych LP. Selection of voxel size and slice orientation for fMRI in the presence of susceptibility field gradients: application to imaging of the amygdala. Neuroimage 2003;19:817–825.

30. Ojemann JG, Akbudak E, Snyder AZ, McKinstry RC, Raichle ME, Conturo TE. Anatomic localization and quantitative analysis of gradient refocused echo-planar fMRI susceptibility artifacts. Neuroimage 1997;6:156–167.

31. Ashburner J, Friston KJ. Voxel-based morphometry—the methods. Neuroimage 2000;11:805–821.

32. Whitfield-Gabrieli S, Nieto-Castanon A. Conn: a functional connectivity toolbox for correlated and anticorrelated brain networks. Brain Connect 2012;2:125–141.

33. Murphy K, Birn RM, Handwerker DA, Jones TB, Bandettini PA. The impact of global signal regression on resting state correlations: are anti-correlated networks introduced? Neuroimage 2009;44:893–905.

34. Birks JS, Harvey RJ. Donepezil for dementia due to Alzheimer's disease. Cochrane Database Syst Rev 2018;6: CD001190.

35. Deardorff WJ, Feen E, Grossberg GT. The use of cholinesterase inhibitors across all stages of Alzheimer's disease. Drugs Aging 2015;32:537–547.

36. Farlow MR, Grossberg GT, Sadowsky CH, Meng X, Somogyi M. A 24-week, randomized, controlled trial of rivastigmine patch 13.3 mg/24 h versus 4.6 mg/24 h in severe Alzheimer's dementia. CNS Neurosci Ther 2013;19:745–762.

37. Wilcock GK, Lilienfeld S, Gaens E. Efficacy and safety of galantamine in patients with mild to moderate Alzheimer's disease: multicentre randomised controlled trial. Galantamine International-1 Study Group. BMJ 2000;321:1445–1449.

38. Wilcock G, Howe I, Coles H, et al. A long-term comparison of galantamine and donepezil in the treatment of Alzheimer's disease. Drugs Aging 2003;20:777–789.

39. Mazza M, Marano G, Traversi G, Bria P, Mazza S. Primary cerebral blood flow deficiency and Alzheimer's disease: shadows and lights. J Alzheimers Dis 2011;23:375–389.

40. Schapiro MB, Pietrini P, Grady CL, et al. Reductions in parietal and temporal cerebral metabolic rates for glucose are not specific for Alzheimer's disease. J Neurol Neurosurg Psychiatry 1993;56:859–864.

41. Alsop DC, Detre JA, Grossman M. Assessment of cerebral blood flow in Alzheimer's disease by spin-labeled magnetic resonance imaging. Ann Neurol 2000;47:93–100.

42. Johnson NA, Jahng GH, Weiner MW, et al. Pattern of cerebral hypoperfusion in Alzheimer disease and mild cognitive impairment measured with arterial spin-labeling MR imaging: initial experience. Radiology 2005;234:851–859.

43. Asllani I, Habeck C, Scarmeas N, Borogovac A, Brown TR, Stern Y. Multivariate and univariate analysis of continuous arterial spin labeling perfusion MRI in Alzheimer's disease. J Cereb Blood Flow Metab 2008;28:725–736.

44. Dai W, Lopez OL, Carmichael OT, Becker JT, Kuller LH, Gach HM. Mild cognitive impairment and Alzheimer disease: patterns of altered cerebral blood flow at MR imaging. Radiology 2009;250:856–866.

45. Yoshiura T, Hiwatashi A, Yamashita K, et al. Simultaneous measurement of arterial transit time, arterial blood volume, and cerebral blood flow using arterial spin-labeling in patients with Alzheimer disease. AJNR Am J Neuroradiol 2009;30:1388–1393.

46. Ding B, Ling HW, Zhang Y, et al. Pattern of cerebral hyperperfusion in Alzheimer's disease and amnestic mild

cognitive impairment using voxel-based analysis of 3D arterial spin-labeling imaging: initial experience. Clin Interv Aging 2014;9:493–500.

47. Nobili F, Vitali P, Canfora M, et al. Effects of long-term Donepezil therapy on rCBF of Alzheimer's patients. Clin Neurophysiol 2002;113:1241–1248.

48. Staff RT, Gemmell HG, Shanks MF, Murray AD, Venneri AA. Changes in the rCBF images of patients with Alzheimer's disease receiving Donepezil therapy. Nucl Med Commun 2000;21:37–41.

49. Venneri A, Shanks MF, Staff RT, et al. Cerebral blood flow and cognitive responses to rivastigmine treatment in Alzheimer's disease. Neuroreport 2002;13:83–87.

50. Stefanova E, Wall A, Almkvist O, et al. Longitudinal PET evaluation of cerebral glucose metabolism in rivastigmine treated patients with mild Alzheimer's disease. J Neural Transm 2006;113:205–218.

51. Uozumi Y, Nawashiro H, Sato S, Kawauchi S, Shima K, Kikuchi M. Targeted increase in cerebral blood flow by transcranial near-infrared laser irradiation. Lasers Surg Med 2010;42:566–575.

52. Rojas JC, Bruchey AK, Gonzalez-Lima F. Low-level light therapy improves cortical metabolic capacity and memory retention. J Alzheimers Dis 2012;32:741–752.

53. Schiffer F, Johnston AL, Ravichandran C, et al. Psychological benefits 2 and 4 weeks after a single treatment with near infrared light to the forehead: a pilot study of 10 patients with major depression and anxiety. Behav Brain Funct 2009;5:46.

54. Nawashiro H, Wada K, Nakai K, Sato S. Focal increase in cerebral blood flow after treatment with near-infrared light to the forehead in a patient in a persistent vegetative state. Photomed Laser Surg 2012;30:231–233.

55. Chetelat G, Desgranges B, de la Sayette V, et al. Dissociating atrophy and hypometabolism impact on episodic memory in mild cognitive impairment. Brain 2003;126:1955–1967.

56. Lustig C, Snyder AZ, Bhakta M, et al. Functional deactivations: change with age and dementia of the Alzheimer type. Proc Natl Acad Sci U S A 2003;100:14504–14509.

57. Sole-Padulles C, Bartres-Faz D, Llado A, et al. Donepezil treatment stabilizes functional connectivity during resting state and brain activity during memory encoding in Alzheimer's disease. J Clin Psychopharmacol 2013;33:199–205.

58. Goveas JS, Xie C, Ward BD, Wu Z, Li W, Franczak M. Recovery of hippocampal network connectivity correlates with cognitive improvement in mild Alzheimer's disease patients treated with donepezil assessed by resting-state fMRi. J Magn Reson Imaging 2011;34:764–773.

59. Li W, Antuono PG, Xie C, et al. Changes in regional cerebral blood flow and functional connectivity in the cholinergic pathway associated with cognitive performance in subjects with mild Alzheimer's disease after 12-week donepezil treatment. Neuroimage 2012;60:1083–1091.

60. Blautzik J, Keeser D, Paolini M, et al. Functional connectivity increase in the default-mode network of patients with Alzheimer's disease after long-term treatment with galantamine. Eur Neuropsychopharmacol 2016;26:602–613.

61. Lorenzi M, Beltramello A, Mercuri NB, et al. Effect of memantine on resting state default mode network activity in Alzheimer's disease. Drugs Aging 2011;28:205–217.

62. Chirles TJ, Reiter K, Weiss LR, Alfini AJ, Nielson KA, Smith JC. Exercise training and functional connectivity changes in mild cognitive impairment and healthy elders. J Alzheimers Dis 2017;57:845–856.

63. Suo C, Singh MF, Gates N, et al. Therapeutically relevant structural and functional mechanisms triggered by physical and cognitive exercise. Mol Psychiatry 2016;21:1645.

64. Wells RE, Kerr CE, Wolkin J, et al. Meditation for adults with mild cognitive impairment: a pilot randomized trial. J Am Geriatr Soc 2013;61:642–645.

65. Dennis EL, Thompson PM. Functional brain connectivity using fMRi in aging and Alzheimer's disease. Neuropsychol Rev 2014;24:49–62.

66. Sommer AP, Bieschke J, Friedrich RP, et al. 670 nm laser light and EGCG complementarily reduce amyloid-β aggregates in human neuroblastoma cells: basis for treatment of Alzheimer's disease? Photomed Laser Surg 2012;30:54–60.

67. De Taboada L, Yu J, El-Amouri S, et al. Transcranial laser therapy attenuates amyloid-beta peptide neuropathology in amyloid-beta protein precursor transgenic mice. J Alzheimers Dis 2011;23:521–535.

68. Grillo SL, Duggett NA, Ennaceur A, Chazot PL. Noninvasive infra-red therapy (1072 nm) reduces beta-amyloid protein levels in the brain of an Alzheimer's disease mouse model, TASTPM. J Photochem Photobiol B 2013;123:13–22.

69. Purushothuman S, Johnstone DM, Nandasena C, Mitrofanis J, Stone J. Photobiomodulation with near infrared light mitigates Alzheimer's disease-related pathology in cerebral cortex—evidence from two transgenic mouse models. Alzheimers Res Ther 2014;6:2.

70. Ando T, Xuan W, Xu T, et al. Comparison of therapeutic effects between pulsed and continuous wave 810-nm wavelength laser irradiation for traumatic brain injury in mice. PLoS One 2011;6:e26212.

71. Wu Q, Xuan W, Ando T, et al. Low-level laser therapy for closed-head traumatic brain injury in mice: effect of different wavelengths. Lasers Surg Med 2012;44:218–226.

72. Iaccarino HF, Singer AC, Martorell AJ, et al. Gamma frequency entrainment attenuates amyloid load and modifies microglia. Nature 2016;540:230–235.

73. McKhann GM, Knopman DS, Chertkow H, et al. The diagnosis of dementia due to Alzheimer's disease: recommendations from the National Institute on Aging-Alzheimer's Association workgroups on diagnostic guidelines for Alzheimer's disease. Alzheimers Dement 2011;7:263–269.

Address correspondence to:
Linda L. Chao, PhD
Center for Imaging of Neurodegenerative Diseases
San Francisco VA Medical Center
4150 Clement Street (114M)
San Francisco, CA 94121

E-mail: linda.chao@ucsf.edu